Research Article **AJCR 2017 1:1**

American Journal of Chemical Research
(ISSN: 2573-0231)

Synthesis of graphene oxide using tea-waste biochar as green substitute of graphite and its application in de-fluoridation of contaminated water

Swapnila Roy

Department of Chemical Engineering, Jadavpur University, 188, Raja S.C. Mullick Road, Kolkata - 700 032, India

ABSTRACT

In the present study, pyrolysis of domestic tea waste was carried out to yield bio-char. The biochar obtained was further used as a substitute for graphite in synthesis of graphene oxide (GO) in the conventional process. GO obtained was further applied for fluoride removal from simulated effluents. The prepared adsorbent was characterized using SEM, XRD and FTIR analysis. Effect of different experimental parameters on the de-fluoridation efficiency of the reported adsorbent was investigated. Data obtained was further used for determination of process isotherms, kinetics and thermodynamics. The regeneration potential of the reported adsorbent was also determined. The experimental results suggested that equilibrium adsorption data was strongly guided by the Langmuir isotherm and pseudo-second-order kinetics. Analysis of process thermodynamics also revealed that the adsorption reaction was spontaneous chemisorption in nature. Significant process parameters including GO dosage, ambient temperature and contact time were optimized using Response surface methodology (RSM) and artificial neural network (ANN). Results of RSM and ANN analysis indicated good correlation between experimentally recorded and theoretically predicted % fluoride removals. Under optimized conditions, fluoride removal efficiency was found to be 98.31%. Therefore, it can be inferred that tea waste derived biochar may be accepted as a sustainable alternative of graphite for GO synthesis. Moreover GO so obtained has immense potential for de- fluoridation of effluents in highly reduced dosage and treatment time.

Keywords: Tea waste; Non-graphite GO; Fluoride removal; Process optimization; Isotherms and kinetics; Chemisorption

***Correspondence to Author:**
Swapnila Roy
Department of Chemical Engineering, Jadavpur University, 188, Raja S.C. Mullick Road, Kolkata - 700 032, India
Email: swapnilaroy @gmail.com

How to cite this article:
Swapnila Roy.Synthesis of graphene oxide using tea-waste biochar as green substitute of graphite and its application in de-fluoridation of contaminated water. American Journal of Chemical Research, 2017, 1:1

eSciencePublisher
eSciPub LLC, Houston, TX USA.
Website: http://escipub.com/

1. Introduction:

Fluorides are widely utilized for in the semiconductor and nanotechnology industries as glass and silica etchants. The prime sources of fluoride in industrial effluents are hydrofluoric acid (HF) and ammonium bi-fluoride (NH_4HF) (Lounici *et al.,* 1997; Roy and Das, 2016a, 2016b). Fluoride has a very high affinity for calcium (Ca) due to the high electronegative character of the former and is therefore strongly attracted by positive calcium ions. Chronic fluoride exposure may result in fluorosis. According to WHO guidelines, the maximum permissible limit of fluoride in drinking water is 1.5 mg L^{-1}. Previous studies have reported various methods such as ion-exchange precipitation, reverse osmosis, electro coagulation, etc. for the de-fluoridation of contaminated water. However, utilization of adsorption technology may be considered as the most appropriate process for treatment of fluoride containing wastewater.

Of all other adsorbents reported so far, graphene oxide (GO) possessing hydrophilic nature and high negative charge density was found to demonstrate efficient adsorption abilities owing to a large number of hydroxyl and epoxy groups present on its basal planes and carboxyl groups bordering its edges (Banerjee *et al.,* 2015). Almost all studies reported so far have synthesized GO from both natural and synthetic graphite (Sierra *et al.,* 2016). However, natural graphite reserves are restricted to few global zones whereas synthetic graphite synthesis from commercial precursors necessitates extremely elevated temperatures (≥ 2500 °C) and therefore is a cost intensive procedure (Sierra *et al.,* 2016). In a recent report, waste biomass has been suggested as a potential precursor material for commercial synthesis of carbonaceous materials owing to their eco-friendly nature, abundant availability in bulk quantities across the world and lower cost and temperature requirements in comparison to conventional graphite (Hu *et al.,* 2010). Carbon materials prepared from waste biomass were been previously applied as adsorption, hydrogen capture, synthesis of biochemicals, etc. (Hu *et al.,* 2010). However, properties of precursor substrate (like purity, crystallinity, homogeneity, etc.) were dependent upon the type of biomass used, the pyrolysis temperature and various other experimental conditions (Mohan *et al.,* 2011; Yuan *et al.,* 2011). Precursor substrate properties were in turn found to exert significant effect on structure and adsorption efficiency of synthesized GO (Inagaki *et al.,* 2011; Wu *et al.,* 2011; Botas *et al.,* 2012; Sierra *et al.,* 2016). Hence, it is highly essential to recognize an appropriate precursor substrate that will substitute graphite in GO synthesis prior to achieving wide scale synthesis of the same from discarded biomass.

This study elucidated a novel route for syntheses of GO using tea waste derived biochar as a green substitute for graphite in conventional procedure. Biochar was prepared from pyrolysis of tea-waste (a domestic waste available in bulk quantities) biomass in a tubular reactor under limited oxygen or at inert atmosphere under high temperatures as described in previous studies (Lehmann *et al.,* 2012; Ahmad *et al.,* 2014) and used as a substitute of graphite in conventional GO synthesis. The GO so synthesized were investigated for its de-fluoridation potential with simulated effluents. The mechanism of de-fluoridation by solid absorbents may usually occur via external mass transfer, adsorption of fluoride ions onto adsorbate surfaces or intra particular diffusion. Depending on the chemical properties of the adsorbent used and the porosity of the internal surfaces of that adsorbent, adsorbed fluoride ions may replace the structural elements constituting the adsorbent moieties.

The structure and morphology of the adsorbent surface were visualized with scanning electron microscopic (SEM) images. The chemical properties of the adsorbent were deciphered from X-ray diffraction (XRD) and Fourier transform infrared (FTIR) spectroscopy. Effect of different process parameters such as adsorbent dose, contact time, reaction temperature, pH and their interactions were investigated in order to understand their impact on the fluoride removal efficiency of the designed adsorbent. Data obtained in batch studies were further subjected for determination adsorption capacity of biochar derived GO as well as analysis of process isotherms. The combined effect of different parameters such as contact time with adsorbent, adsorbent dose and temperature was considered for both RSM and ANN study. The significant process parameters were optimized using Central Composite Design (CCD) feature of Response surface methodology (RSM). The CCD results were further mod-

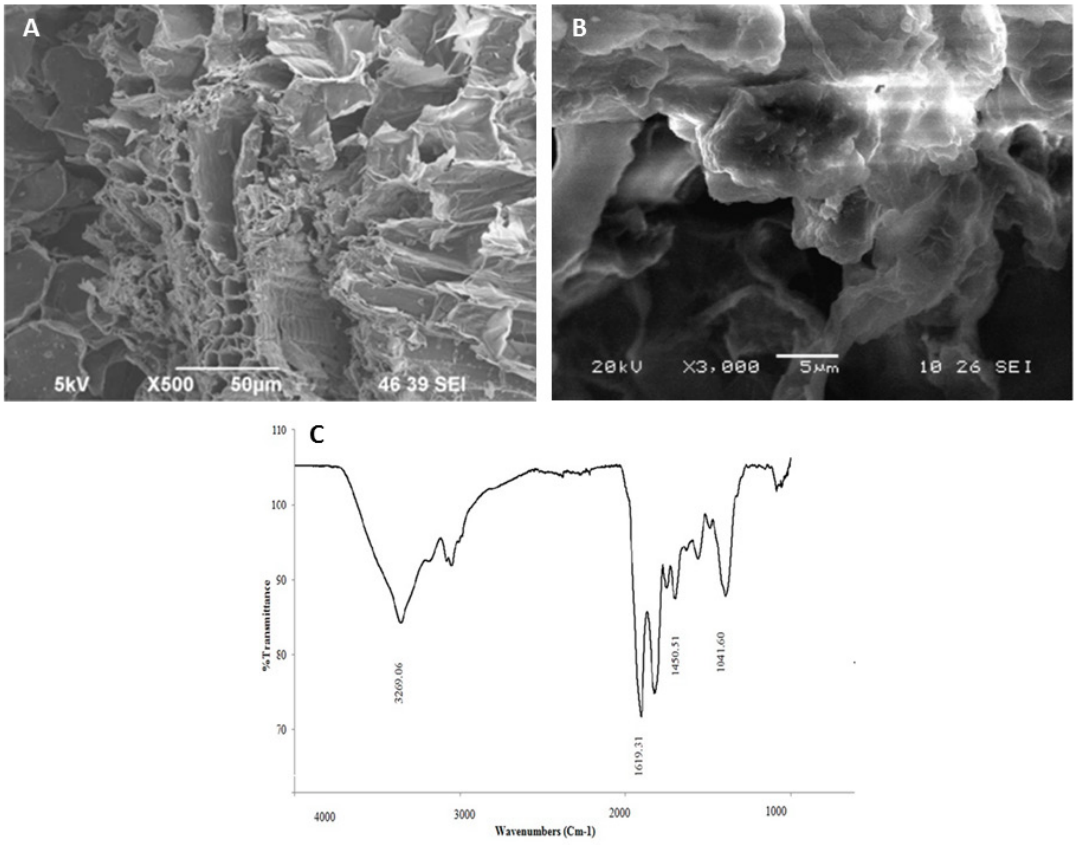

Figure.1: Characterization of GO (A: SEM image of tea waste; B: SEM image of GO; C: FTIR spectrum of GO).

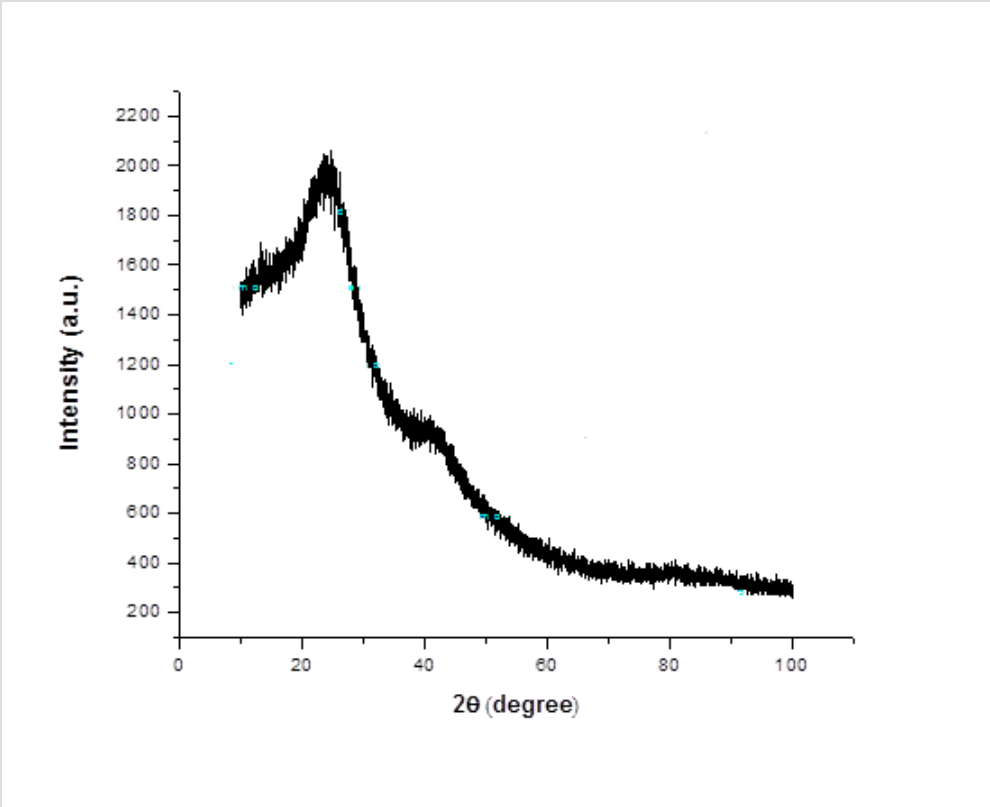

Figure 2: XRD of GO

Table 1. Investigating different isotherm parameters for fluoride adsorption by chemically modified biochar

Models	Parameters	Description	Unit	Dose (g L^{-1})			
				2	5	7.5	10
Langmuir	C_e	Equilibrium fluoride concentration in solution	mg L^{-1}	8.94	46.93	320.18	322.25
	q_e	Theoretical maximum adsorption capacity	mg g^{-1}	20.30	22.23	23.76	24.56
	Q_0	Maximum monolayer coverage capacity calculated from slope of C_e/q_e vs. C_e plot.	mg g^{-1}	22.35	31.25	34.48	52.47
	b	Langmuir coefficient of energy of adsorption calculated from intercept of C_e/q_e vs. C_e plot.	L mg^{-1}	0.93	0.94	0.96	0.99
	R^2	Correlation coefficient		0.987	0.989	0.994	0.999
Freundlich	n_f	Adsorption intensity calculated from slope of $ln\ q_e$ vs. $ln\ C_e$ plot		5.27	12.52	49.85	55.48
	K_f	Freundlich coefficient of adsorption capacity calculated from intercept of $ln\ q_e$ vs. $ln\ C_e$ plot	mg g^{-1}	12.62	15.62	18.87	20.52
	R^2	Correlation coefficient		0.973	0.987	0.901	0.9805
Temkin	B_T	Coefficients of heat of adsorption calculated from slope of q_e vs. $ln\ C_e$ plot at operational temperature T (308 K)	J mol^{-1}	3.62	2.37	2.12	2.01
	K_T	Temkin equilibrium binding constant calculated from intercept of q_e vs. $ln\ C_e$ plot at operational temperature T (333 K)	L g^{-1}	1.1 E+12	1.13E+9	1.23E+6	3.24E+5
	R^2	Correlation coefficient		0.982	0.956	0.961	0.9815

Table 2. Analysis of kinetic parameters for fluoride adsorption by chemically modified biochar

Models	Parameters	Description	Units	Temperatures (°C)			
				35	45	55	60
Pseudo first order $\log(q_e - q_t) = [\log q_e - \frac{k_1}{2.303} t]$	k_1	Pseudo-1st order rate constant obtained from linear plots of *log* $(q_e - q_t)$ vs. *t*.	min^{-1}	0.0019	0.0021	0.0025	0.0025
	q_e (cal)	Quantity of fluoride adsorbed at equilibrium	mg g^{-1}	2.53	8.39	6.59	9.79
	R^2	Correlation coefficient		0.614	0.829	0.879	0.892
Pseudo second order $\frac{t}{q_t} = \frac{1}{k_2 q_e^2} + \frac{t}{q_e}$	k_2	Pseudo-2nd order rate constant determined from plot of t/q_t vs. *t*.	mg g^{-1} min^{-1}	0.03	0.04	0.04	0.03
	q_e	Quantity of fluoride adsorbed at equilibrium	mg g^{-1}	22.22	24.39	25.64	25.64
	R^2	Correlation coefficient		0.988	0.971	0.991	1.000

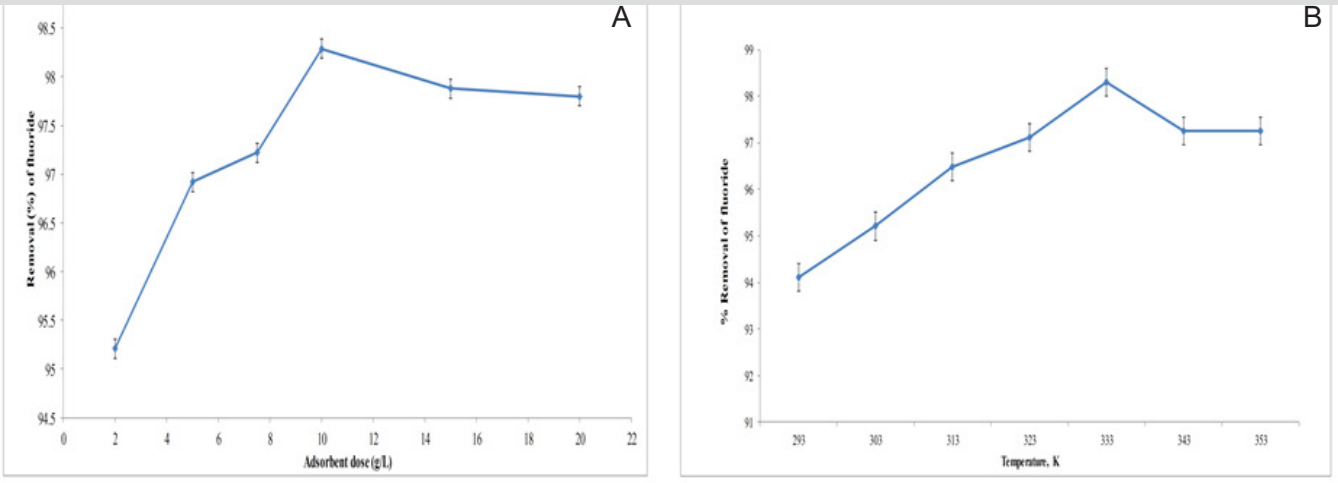

Figure 3: Results of batch study. (A: Effect of adsorbent dose on de-fluoridation by GO where C0 = 50 mg L−1, agitation speed = 150 rpm, T = 333 K and adsorbent dose = 10 g L-1); B: Effect of temperature on de-fluoridation by GO where C0 = 50 mg L−1, agitation speed = 150 rpm, adsorbent dose=10 g L−1 and contact time: 120 min).

eled with artificial neural network (ANN) coded by different back propagation (BP) algorithms.

2.0 Experimental Design:

2.1 Materials and Instruments:

Concentrated sulphuric acid (98 wt. %) hydrogen peroxide (30 wt. %), Sodium Fluoride and all other reagents used in this study were purchased from Merck, India (reagent grade) and used as obtained. Tea leaves were also obtained commercially. Experimental fluoride solutions (stock and dilutions) were all prepared with ultrapure distilled water. As and when required, pH adjustments were made with 0.1N HCl or 0.1 M NaOH.

2.2 Preparation of GO:

Tea waste was used as precursor substrate for preparation of adsorbent (bio-char) in a process described by Kloss *et al*. (2012). GO was prepared from tea waste by pyrolysis process under inert atmosphere (nitrogen atmosphere). Firstly, dried tea waste powder taken in a ceramic crucible was placed in a tubular reactor and charred at 673 K in nitrogen atmosphere for 30 min. Afterwards, the resultant GO was cooled, ground and sieved to obtain a homogenous powder of particle size was less than 0.2 mm.

GO was synthesized using Hummer's method with modifications (Hummers and Offeman, 1958). For this, concentrated H_2SO_4 was added to dried biochar powder. Further, $NaNO_3$ (0.8 g) was added to the acidic bichar slurry. Then $KMnO_4$ (2.5 g) was added to the mixture (very slowly) with continuous stirring. The mixture was then kept aside at room temperature for 2 hours. Then temperature was gradually increased from 323 K to 373 K. Finally, 30% H_2O_2 was added to the heated mixture until the color of the same turned bright yellow. The colloidal solution was then ultrasonicated for 15 min and filtered. The residue was washed repeatedly washed with 5% aqueous HCl for removal of metal ions and further washed with distilled water for removal of excess acid present (if any). The resulting GO powder was dried in oven, ground, sieved and stored for later use.

2.3 Characterization of GO:

2.3.1 Scanning electron microscopy (SEM):

The Scanning Electron Microscopy of the sample was performed using JEOL-JSM-6360 (Jeol, Japan). SEM analysis was conducted to study the changes in surface morphology such as smoothness and roughness of GO. Samples were coated with gold prior to recording of images for rendering the same conductive.

2.3.2 XRD (X-ray diffraction):

X-ray diffraction analysis of GO was conducted using X-ray diffractometer equipment (Bruker, D8 Advance, Germany) with a Cu Kα radiation at an accelerating voltage 40 kV and emission current 30 mA in the range of diffraction angle $2\theta = 10 - 80^{o}$. The XRD analysis was conducted to investigate the interlayer spacing of the prepared sample.

2.3.3 FTIR(Fourier Transformed Infrared Spectroscopy):

The infrared spectra of the adsorbent were recorded using Fourier Transform Infrared Spectrometer (Perkin Elmer Spectrum, United Kingdom) in transmittance mode. The KBr pressed pellet technique was used to record the spectrum. Samples were cast into pellets with potassium bromide (KBr) and scanned in the mid IR range of 1000-4000 cm^{-1}.

2.4 Physico-chemical properties of GO:

The physicochemical properties of the prepared GO were estimated using standard procedures (Jun *et al*., 2010).

2.4.1 Determination of Bulk Density of GO:

Dry empty 10 ml centrifuge tubes was cleaned and weighed (W_1).The same tubes were then filled with the prepared GO powder and weighed (W_2) again. The difference in the initial and final weights denoted the weight of GO powder in tube. The bulk density was then estimated using the following equation:

$$\text{Bulk Density} = (W_2 - W_1)/(\text{Volume of centrifuge tube}) \quad \ldots\ldots\ldots\ldots\ldots\ldots\ldots (1)$$

2.4.2 Determination of Moisture Content:

Empty crucibles was dried at 383 K, cooled in a desiccator and weighed (W_1). Then a known weight of GO was with added to the crucible and weighed (W_2). The crucible containing GO was

Table 3: Details of RSM and ANN analysis

Details of Response Surface Methodology (CCD) Optimization						Details of Artificial Neural Network Modeling				
Factors	Levels			Star point α = 2.37		Algorithm selected for hidden layer	Selected Functions			Correlation coefficient (R)
	Low (-1)	Central (0)	High (+1)	-α	+α		Output Layer	Transfer 1	Transfer 2	
Adsorbent dose ($g\ L^{-1}$)	10.0	15.0	20.0	6.6	23.4	Levenberg-Marquardt backpropagation	Trainlm	Poslin	Purelin	0.962
Contact time (min)	40	80	120	12.7	147.2	Resilient backpropagation	Trainrp	Poslin	Purelin	0.92
						Conjugate gradient backpropagation with Polak-Ribiere updates	Traincgp	Poslin	Purelin	0.608
Temperature (K)	308	320.5	333	299.4	2.34	Scaled conjugate gradient backpropagation	Trainscg	Poslin	Purelin	0.77
						Gradient descent with momentum and adaptive learning rate backpropagation	Traingdx	Poslin	Purelin	0.43

Run No.	Adsorbent dose($g\ L^{-1}$)	Contact time	Temperature	% Fluoride Removal
1	20	120	333	93.23
2	15	12.7	320.5	90.06

3	6.6	80	320.5	91.49
4	15	80	341.5	96.24
5	23.4	80	320.5	97.32
6	15	80	320.5	95.89
7	15	147.2	320.5	96.49
8	10	40	308	89.31
9	10	40	333	93.34
10	20	40	333	96.91
11	15	80	320.5	96.89
12	15	80	320.5	96.89
13	20	120	308	96.21
14	15	80	320.5	96.89
15	10	120	333	98.31
16	15	80	320.5	96.89
17	15	80	299.4	94.31
18	15	80	320.5	97.89
19	10	120	308	96.56
20	20	40	308	95.35

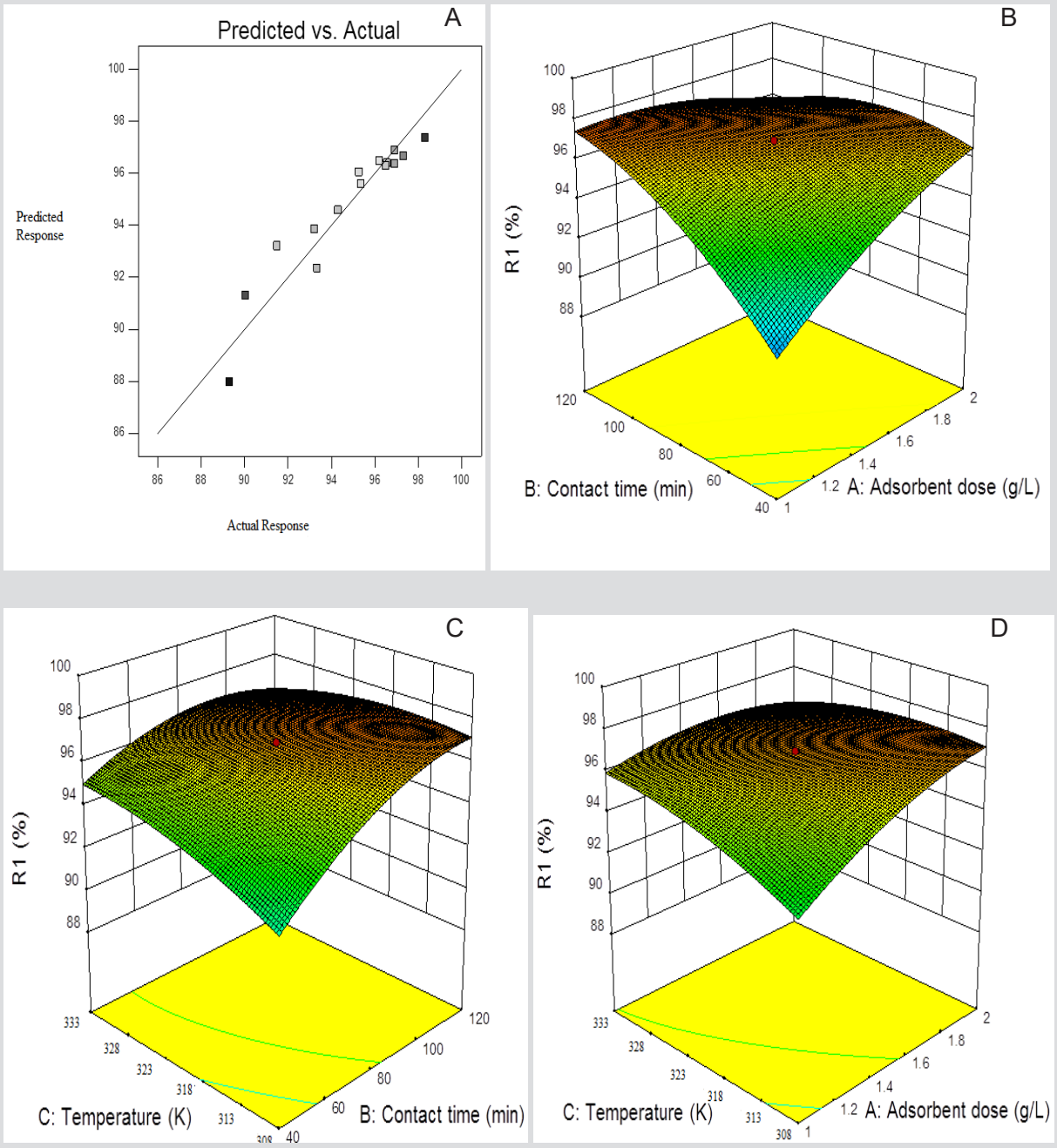

Figure 4: Results of RSM analysis (A: The graph showing predicted removal % vs actual removal% of fluoride by GO; B: Response surface plot showing interaction effect of dosage and contact time; C: Response surface plot showing interaction effect of temperature and contact time ; D: Response surface plot showing interaction effect of temperature and dosage).

then dried in an oven at 383K. This weight was then constantly monitored every 30 minutes until the weight became constant. Then the crucible with GO was cooled in a desiccator and reweighed (W_3). The difference in initial and final weights of GO was used to calculate the moisture content (X_o) of GO prepared from tea waste.

$X_0=(W_2-W_3)/(W_2-W_1)X100$ ..... (2)

2.4.3Yield of GO:

After pyrolysis of tea waste, the GO obtained was cooled and weighed. The percentage yield of GO was then calculated by applying the following formula:

% yield of GO= (Weight of GO)/(Weight of raw material) ..... (3)

2.4.4 Porosity Determination:

The porosity and pore volumes of GO were estimated using the following formulas:

$$\text{Porosity} = \frac{pore\ volume}{total\ volume}$$

Pore volume= (Bulk density of GO)/(Density of water)

Porosity = (Bulk density of GO)/(Density of water X Total volume) ..... (4)

2.5 Batch adsorption studies:

In this case, 100 mL fluoride solutions of 50 mg L^{-1} concentration were taken in 250 mL PTFE (Polytetrafluoroethylene) conical flasks. The predetermined amounts of adsorbent were added to each solution. Then the flasks were agitated at 150 rpm in an incubator shaker (INNOVA 4430, New Brunswick Scientific, Canada) at different temperatures. The effects of varying contact time, adsorbent dose and reaction temperatures on the adsorption of fluoride were investigated. The residual amount of fluoride in each experiment was estimated by using ion-meter (Thermo Scientific Orion ion-meter, USA).

The percent removal (%) of fluoride is determined by using the following equation:

$$\text{Percentage Removal (\%)} = \frac{C_i - C_0}{C_i} \text{ x100} \quad \text{..... (5)}$$

Where, C_i and C_0 denoted the initial and final fluoride concentrations (mg L^{-1}) respectively.

2.6 Isotherm, Kinetics and Thermodynamic Study:

2.6.1 Adsorption Isotherms:

The Freundlich isotherm constants were estimated using the following equation:

$LnQ_e = lnK_F + (1/n)\ lnC_e$ ..... (6)

Where, Q_e was the amount of fluoride adsorbed at equilibrium, and K_F and n were Freundlich constants indicating adsorption capacity and adsorption intensity respectively.

In case of Langmuir isotherm, the following equation was used:

$$\frac{C_e}{Q_e} = \frac{C_e}{q_m} + \frac{1}{K_L q_m} \quad \text{..... (7)}$$

Where, Q_e was the amount of fluoride adsorbed at equilibrium (mg L^{-1}), C_e was the concentration of fluoride in the aqueous phase at equilibrium (mg L^{-1}). K_L and q_m denoted the Langmuir constants related to energy of adsorption and the adsorption capacity respectively.

Temkin isotherm was guided by the following equation:

$$q_e = B \ln A_T + B \ln C_e \quad \text{..... (8)}$$

Where, A_T denoted Temkin isotherm equilibrium binding constant (L g^{-1}), b_T denoted Temkin isotherm constant, R was the universal gas constant (8.314 J mol^{-1} K^{-1}), T denoted temperature (298 K) and B, a constant indicating heat of adsorption (J mol^{-1}) was calculated as follows:

$$B = RT / b_T$$

2.6.2 Adsorption kinetics:

Adsorption kinetic was estimated using pseudo 1st order and 2nd order kinetics equation.

The pseudo 1st order rate constant was estimated using the following equation:

$$\frac{dq_t}{dt} = k_1(q_e - q_t) \quad \text{..... (9)}$$

Where, q_e indicated fluoride adsorbed at equilibrium per unit weight of adsorbent (mg g^{-1}), q_t denoted the amount of fluoride adsorbed at any

Table 4: Comparative analysis of previously reported adsorbents with chemically modified biochar synthesized in this study:

Sorbent	Maximum adsorbent capacity (mg g^{-1})	Isotherm	Reference
Activated Carbon prepared from Rice straw	18.9	Langmuir	Daifullah *et al*., 2007
Activated Carbon prepared from *Morringa indica*	0.2314	Langmuir	Karthikeyan *et al*., 2007
Activated carbon prepared from *Acacia farnesiana*	2.622	Freundlich	Hanumantharao *et al*., 2011
Activated carbon prepared from Pithacelo biumdulce	1.9333	Freundlich	Emmanuel *et al*., 2008
Activated carbon prepared from *Anacardium occidentale*	1.95	Langmuir	Alagumuthu and Rajan, 2010a
Activated carbon prepared from *Arachis hypogia*	14.79	Freundlich	Alagumuthu and Rajan, 2010b
Activated carbon prepared from *Cynodon dactylon*	4.755	Langmuir	Alagumuthu *et al*., 2011
Activated carbon prepared from peanut shells	2.3	Langmuir	Hernández-Montoya *et al*., 2012
Graphene	48.31	Langmuir	Li *et al*., 2011
Chemically modified Biochar	*52.47*	*Langmuir*	*Present study*

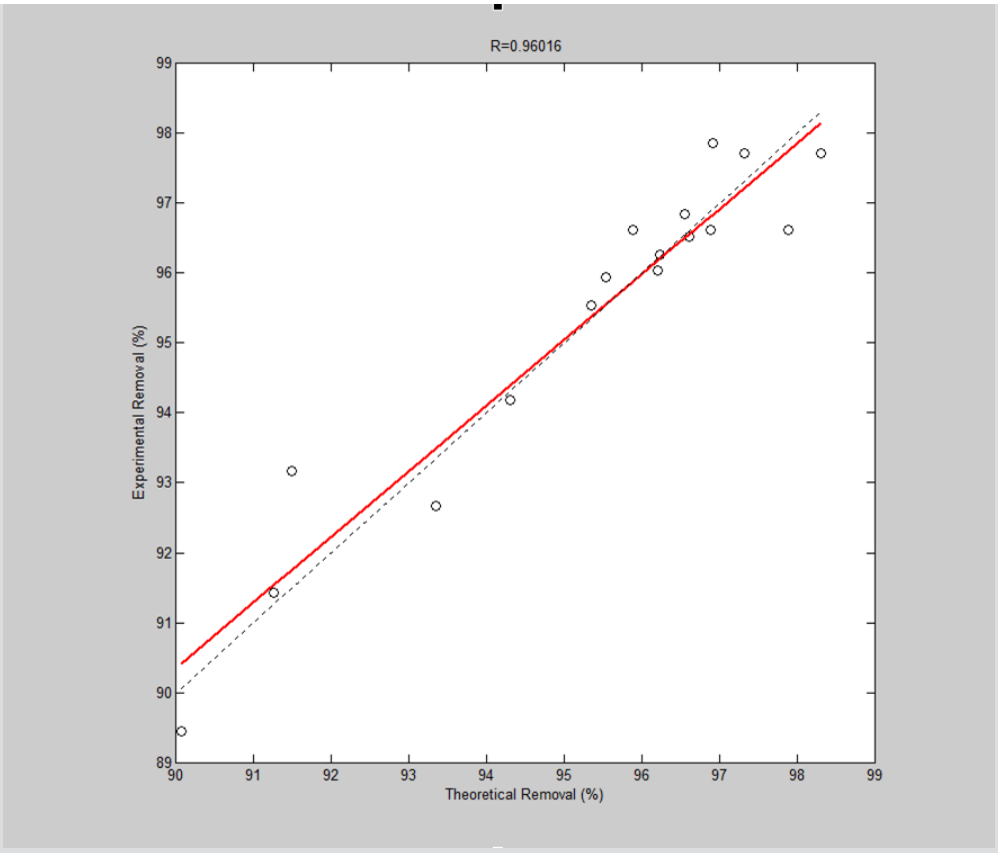

Figure 5: Graphical plot of theoretical % fluoride removal vs. experimental % fluoride removal from ANN analysis

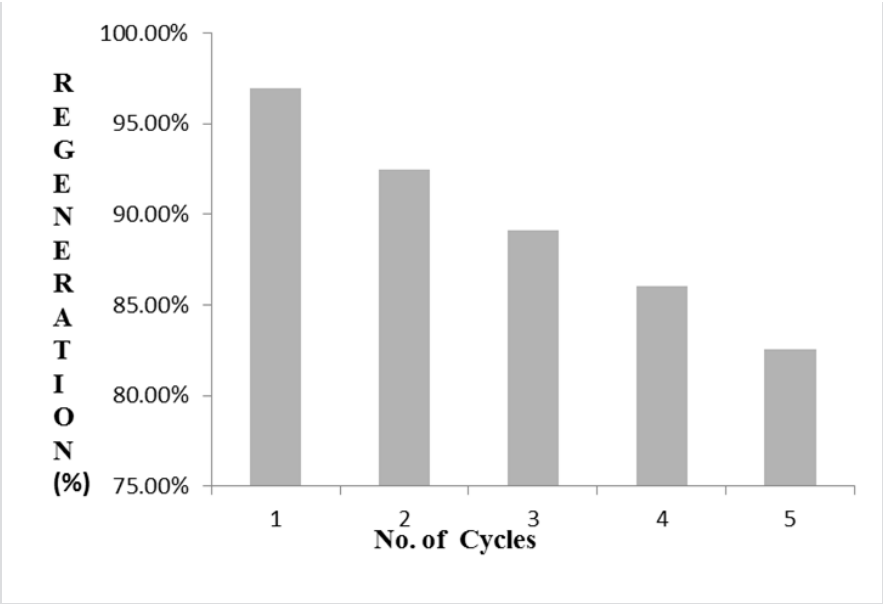

Figure 6: % fluoride removal by regenerated GO

Supplementary Table 1: Removal of Fluoride at different pH of the solution by chemically modified biochar

Sl No.	pH of solution	% Removal
1	2	98.28
2	4	95.29
3	6	91.25
4	8	89.38
5	10	87.28
6	12	82.1

Supplementary Table 2: Thermodynamic parameters for the adsorption of fluoride by chemically modified bio-char:

Serial No.	T(K)	ΔG^0 (KJ mol^{-1})	ΔH^0 (KJ mol^{-1})	ΔS^0 (J mol^{-1} K^{-1})
1	298	-8.93	28.3413	97.28
2	308	-10.23		
3	318	-12.45		
4	323	-13.12		
5	333	-14.45		
6	353	-12.35		

Supplementary Table 3: Analysis of variance for the response surface quadratic model for adsorption of fluoride by chemically modified biochar

Parameters	GO
p value (Prob>F)	0.0003
F value	12.21
R^2	0.9166
Adjusted R^2	0.8416

instant (mg g^{-1}) and k_1 was the rate constant (min^{-1}).

Integrating at these conditions as t=0 and q_t=0 to t=t and q_t=q_t, the final equation could be expressed as:

$$\text{Log}(q_e - q_t) = \log q_e - \frac{k_1 t}{2.303} \quad \text{..... (10)}$$

The pseudo 2nd order rate constant was derived from the following equation:

$$\frac{t}{q_t} = \frac{1}{k_2 q_e 2} + 1/q_e(t) \quad \text{..... (11)}$$

Where, k_2 denoted the pseudo 2nd order rate constant of adsorption (g mg^{-1} min^{-1}) and q_e and q_t were the amounts of fluoride adsorbed (mg g^{-1}) at equilibrium and at time t respectively.

2.6.3 Adsorption thermodynamics:

Thermodynamic parameters calculated included changes in Gibbs free energy (ΔG^0; kJ mol^{-1}), enthalpy (ΔH^0; kJ mol^{-1}) and entropy (ΔS^0; J mol^{-1} k^{-1}). These parameters were calculated as follows:

$$K_c = \frac{C_a}{C_e} \quad \text{..... (12)}$$

$$\Delta G^0 = -RT \ln K_c \quad \text{..... (13)}$$

$$\Delta G_0 = \Delta H^0 - T\Delta S^0 \quad \text{..... (14)}$$

Where, K_c was the coefficient of distribution for the adsorption; C_a was fluoride adsorbed per unit mass of the adsorbent (mg L^{-1}) and C_e was equilibrium concentration of adsorbate in aqueous phase (mg L^{-1}), R was universal gas constant (8.314 J mol^{-1} K^{-1}) and T was absolute temperature (K)

2.7 Response surface methodology for optimization of adsorption parameters:

Three independent process variables (adsorbent dose, temperature and contact time) were considered for optimization of the process parameter for efficient removal of fluoride from solution. Design Expert Version 9.1.6 (Stat Ease, USA) was used to optimize the values of the chosen independent parameters. The coefficients of correlation and the quadratic model equation were generated through the model software and validated by the experimental data obtained. The percent removal of fluoride was considered as the response of the system. Statistically the prediction of the optimum condition was obtained by following the quadratic equation:

$$Y = \beta_0 + \sum_{i=1}^{k} \beta i\, xi + \sum_{i=1}^{k} \beta ii\, xi2 + \sum_{i=1} \sum_{j=i+1} \beta ij xi xj + \varepsilon \quad \text{.....(15)}$$

Where, Y was the response (i.e. dependent variable) of the process, β_0 was the constant coefficient, β_i, β_{ii} and β_{ij} were coefficients of linear, quadratic and interaction effect respectively, x_i and x_j denoted factors (independent variables) and ε represented error.

2.8 ANN modeling:

Artificial neural network (ANN) is a combined mathematical and statistical tool applied for modeling of different experimental parameters. MATLAB 7 (The Mathworks, Inc.,Ver. 7.0.1) was selected to develop the ANN model using neural network toolbox. Three input layers were chosen as input layers i.e., independent variables and the output layers acted as dependent variable. For this study, temperature, adsorbent dose and contact time were chosen as independent variables and removal efficiency was chosen as dependent variables. The data collected from batch experiments were provided as system input. After several number of training trials, the best neural network model was chosen. For ensuring good performance of the model, both performance goal and minimum performance gradient were considered in this study.

3. Results and Discussion:

It was observed that porosity was 0.62, yield 52.15%, bulk density 0.8 g cm^3 and moisture content 5.6% of the synthesized GO.

3.1 Characterization of GO:

The prepared GO was characterized by SEM and XRD. From SEM images shown in , it was observed amorphous and heterogeneous layer structure of tea waste chars. On comparing SEM images of tea waste (**Figure 1A**) and GO synthesized from tea waste bio char (**Figure 1B**) interesting morphological changes were observed. From phenomenological point of view, a gradual release of different volatile compounds occurred as the temperature increased during a high rate

of heating. Finally, characteristic thin wrinkled overlying sheet like GO particles were obtained. These may be the result of secondary product formation from the precipitation of volatile gases. From XRD analysis (figure not shown) it was observed that characteristic diffraction peaks of 2θ were obtained at 30.870, corresponding to the interlayer spacing (d002) of 0.3363 nm.

FTIR spectra of the GO sample have been shown in **figure 1C**. The FTIR spectra of tea waste bio-char derived GO exhibited a peak around 1041 cm^{-1}, attributed to C-O stretching of carbohydrate-like substances and peak around 1470 cm^{-1}, attributed to C-O stretching of phenolic, carboxylic, and alcohol groups. The peak observed around 1619 cm^{-1} in the FTIR spectra was assigned to the asymmetric C-O groups. The broad, intense peak at 3269 cm^{-1} was observed, attributed to O–H stretching vibrations due to the presence of trapped water molecules between the layers or due to the O–H stretching mode of intercalated water.

3.2 Batch study

3.2.1 Effect of Adsorbent dose:

Within the experimental range of adsorbent dose (2-20 g L^{-1}), percent removal of fluoride firstly increased (upto10 g L^{-1}), then decreased as observed from **figure 2A**. The adsorbent dose in the range of 2-20 g L^{-1} de-fluoridation efficiency increased due to the number of ions increased on the adsorbent surface as the attractive force between adsorbate ions and adsorbent. While increasing dosage of adsorbent higher than 10 g L^{-1}, there was reduction in de-fluoridation on the adsorbent surface because surface of adsorbent was saturated by adsorbate ions, and in that case the repulsive force between fluoride ions and adsorbent surface occurred. So it can be inferred that GO can be used as effective adsorbent for de-fluoridation in water.

3.2.2 Effect of pH

The solution pH is significant monitoring parameter, driving an adsorption process. In present investigation, the effect of pH on removal efficiency of fluoride was experimented. The results of the pH study was represented in **Supplementary Table 1**. It was observed that rate of removal efficiency was decreased with an increase in pH of fluoride solution and maximum efficiency was found at around pH 2.0 (98.2%). Further decrease in pH (<2), did not remarkably change fluoride removal capacity. It can be explained that GO retained its high adsorption efficiency at acidic pH may be due to electrostatic interaction between cationic surface with negatively charged fluoride. As pH increased, the adsorption capacity reduced may be due to deprotonation of fluoride in alkaline medium in presence of excess OH- ions which may compete with negatively charged fluoride ion.

3.2.3 Effect of temperature :

In this experiment, it was observed that with increasing temperature, the removal efficiency of fluoride increased sharply at 333K and decreased with further rise in temperature as shown in **figure 2B**. With increase in temperature, the attractive force between adsorbent and fluoride ions increased, resulting in an increase in the adsorption capacity of GO. Hence, a decrease in the residual amount of fluoride ions was also observed. Above 333 K the amount of residual fluoride was found to increase gradually.

3.3 Adsorption isotherm:

From **Table 1,** it was evident that R^2 value of Langmuir isotherm model (0.999) was higher than that of Freundlich (0.9805) and Temkin model (0.9815). Hence, Langmuir model showed good agreement on de-fluoridation onto GO in comparison to Freundlich and Temkin model in present work. This also indicated that the surface of GO was homogeneous in nature. With increase in temperature, adsorption capacity of GO was found to improve which in turn implied that the process was endothermic in nature.

3.4 Adsorption kinetics:

From the results obtained, it was observed in **Table 2** that pseudo second order kinetics study were well fitted than pseudo first order reaction. From the pseudo second order kinetic reaction it was observed that adsorption capacity of GO was dependent on available binding site. The value of k_2 and q_e were calculated from the intercept and slope of plot of t/

q_t against t (Figure not shown). The value of R^2 for 25, 50 and 75 mg L^{-1} of fluoride were 0.981, 0.999 and 0.983, respectively and q_e (mg g^{-1}) were 26.290, 28.72 and 29.78 respectively. The value of R^2 for pseudo-second-order was greater than pseudo-first-order process suggesting that de-fluoridation by GO followed pseudo 2^{nd} order kinetics.

3.5 Thermodynamic study

In order to determine the feasibility of reaction, the thermodynamic parameters such as Gibbs free energy (ΔG°), enthalpy (ΔH°) and entropy (ΔS°) was estimated **Supplementary Table 2**. ΔH° and ΔS° were estimated by slope and intercept from the plot of ln K_c vs. T^{-1}. The values of ΔG° were negative at all temperatures, implied that the adsorption process was feasible and spontaneous in nature. The decrease in the value of ΔG° with increasing temperature indicated that adsorption of fluoride by GO was higher at high temperature. The positive value of ΔH° (28.3413 kJ mol^{-1}) indicated that the adsorption process was endothermic. ΔH° found as 28.3413 kJ, which implied that de-fluoridation onto GO followed physicochemical process. The positive value of ΔS° (97.28 J mol^{-1} K^{-1}) showed the affinity of fluoride towards GO resulted in an increased randomness at the solid-liquid interface during adsorption.

3.6 Estimation of response surface for maximum fluoride removal:

The results of the 20 experiments performed as per CCD analysis shown in **Table 3.** The maximum fluoride removal is obtained 98.31% at 120 min contact time, at 373 K and 10 g of adsorbent. The response variable which was expressed as a function of independent variables defined in multiple regression model (Hamsaveni *et al*., 2001; Korbahti *et al*., 2008; Garg *et al*., 2009), developed by Design Expert software is expressed in the form of different numerical factors in equation (16)given below:

$$\%\ \text{Removal of fluoride } (R_1) = +97.84 + 1.32*A + 1.92*B + 0.88*C - 0.85*AB - 0.12*AC - 0.070*BC - 0.75*A^2 - 0.96*B^2 - 0.27C^2 \quad (16)$$

Where A represented adsorbent dose (g L^{-1}), B denoted contact time (min) and C indicated reaction temperature (K). It is observed that A, B, C, B^2, C^2 were significant model terms. The fitness of the model was verified by the correlation coefficient (R^2) between the experimental and model predicted values of the response variable (**Figure 3A**). Statistically R^2 value of 0.9166 indicated that the model was statistically significant. A coefficient of variance indicated reliability of the data obtained by performing the experiment. The ANOVA results of the quadratic model suggested that the model was highly significant, as it was evident from F value (12.21) with a low probability value (**Supplementary Table 3**). The high R^2 value of 0.9166 implied that the regression model was statistically significant. A coefficient of variance of 1.06% suggested better precision and reliability of the data obtained by performing the experiments while a non-significant lack of fit value (more than 0.05) implied the validity of the quadratic model. Overall, the ANOVA analysis indicated the applicability of the model to predict the removal efficiency of fluoride by GO within the limits of the experimental factors.

3.7 Effect of interaction of process variables:

3.7.1 Effect of variation in dosage and contact time:

The response surface plot shown in **figure 3B** depicted the interaction effects of the independent variables (reaction time and adsorbent dose) on the removal of fluoride. According to the response surface plot of figure 3B , removal efficiency increased with increasing dose of adsorbent and time of reaction. Maximum removal efficiency was 98.31%, which was obtained with 120 min adsorption time and dosage of 10g L^{-1}. The observations revealed that after 120 min, removal rates of fluoride were diminished, which may have been due to saturation of the adsorbent surface sites.

3.7.2 Effect of variation in temperature and contact time:

The effect of different temperature and reaction time were essential to study the effective removal of fluoride. It was illustrated in the contour plot shown in **Figure 3C**. It was observed that both the independent process variables were important on removal of fluoride ion from solution. From this response surface plot, a maximal removal efficiency was obtained at 333 K temperature, 120 min contact time. As the tem-

perature increased from 298-373 K, the fluoride uptake capacity increased for GO indicating that at higher temperature with higher contact time, the percentage of adsorbed fluoride on the adsorbent surfaces increased and as a result of which removal of fluoride increased. At the end of 120 min of adsorption process, it was clearly observed that the removal efficiency was maximum at that point and beyond that point, density of fluoride ion increased in solution with increasing reaction time.

3.7.3 Effect of variation in dosage and temperature:

It was observed that percentage of fluoride removal increased on increasing the temperature from 298 K to 373 K and also increased with increasing dose (figure not shown). From this phenomena, it was suggested that higher values of fluoride removal may be obtained by increasing in temperature and also with increasing adsorbent dose. As adsorbent dose increased, the % removal of fluoride increased which may be due to the attractive forces between fluoride ion and adsorbent. As adsorbent dose of the solution increased, the charge density of adsorbent surface increased and as a result electrostatic force of attraction between the fluoride ions and soil surface increased. From this plot, a maximal removal efficiency of 98.31% was achieved at 10 g L^{-1} of adsorbent dose, at 333 K.

3.8 Validation of RSM:

$$\frac{\partial R1}{\partial A} = 1.32 - 0.85B - 0.12C - 1.5A \quad \ldots\ldots\ldots\ldots\ldots (17)$$

$$\frac{\partial R1}{\partial B} = 1.92 - 0.85A - 0.07C - 1.92B \quad \ldots\ldots\ldots\ldots\ldots (18)$$

$$\frac{\partial R1}{\partial C} = 0.88 - 0.12A - .54C \quad \ldots\ldots\ldots\ldots\ldots (19)$$

$$\frac{\partial^2 R}{\partial A^2} = -1.5;\ \frac{\partial^2 R}{\partial B^2} = -1.92;\ \frac{\partial^2 R}{\partial C^2} = -0.54$$

As all the second order derivative were negative, it signified that maximization technique can be applied for this study and for that equations (17 – 19) were equated to zero.

Under this condition, A, B, and C were estimated to be 10.2 g L^{-1}, 119.89 min, and 332.8 K, respectively, and % de-fluoridation obtained to be 98.308% for 100 ml of fluoride contaminated solution.

To support the optimized data given by numerical modeling, confirmatory experiments were performed with the parameters as suggested by the model (Dosage 10.2 g L^{-1}; temperature 333 K; contact time 120 min). The corresponding removal efficiency in optimum conditions was found as 98.31% experimentally. The difference between the removal efficiency in theoretical and experimental conditions was very low confirmed the validity of response surface methodology.

.3.9 Artificial Neural Network

Here mathematical software (MATLAB 7) was applied to design the neural network model (Lee *et al*., 1998; Chu, 2003; Yetilmezsoy and Demirel, 2008) from the experimental data. The removal efficiency (%) of fluoride was selected as the experimental response or output variable. The network which gave a coefficient of correlation (R) between the predicted and experimented results approx.1 was considered to be a perfect model and was hence selected. Linear transfer function 'POSLIN' was selected for the input to hidden layer mapping while purely linear transfer function 'PURELIN' was selected for the hidden layer to the output layer mapping. The correlation coefficient (R) was estimated in each case. The regression plot of the trained network was represented in **Figure 4. Table 3** showed that the 'Levenberg-Marquardt backpropagation (Trainlm)' algorithm with 'poslin' transfer function provided satisfactory result in comparison to other tested algorithms like 'Scaled conjugate gradient (Trainscg)', 'Conjugate gradient backpropagation with Polak-Ribiere updates (Traincgp)', 'Resilient backpropagation (Trainrp)' and Gradient descent with momentum and adaptive learning rate backpropagation (Traingdx)' algorithm.. The developed network model was verified for its ability to predict the response of experimental data (Figure 4).

3.10 Regeneration of GO:

As the tea waste biochar derived GO demonstrated higher de-fluoridation efficiency (98.31%),

so its desorption study was determined by 5 adsorption–desorption cycles. The present adsorption-desorption study was carried out with 100 ml of 50 $mg \cdot L^{-1}$ of synthetic fluoride solution at the beginning of each cycle. The study was investigated with 1% NaOH as desorbing agent. The adsorption capacities of each cycle were 96.92%, 92.46%, 89.13%, 86.01%, and 82.53% . These experimental results (**Figure 5**) represented that tea waste biochar derived GO could be successfully be reused repeatedly for de-fluoridation of contaminated water.

3.11 Comparative analysis of the adsorbent with previous study

It was observed from **Table 4** that the GO had better adsorbent properties in comparison to other adsorbents reported in previous studies.

4. Conclusion:

The present study established for the first time, the conveniently procurable domestic tea waste derived biochar as a sustainable alternative for graphite in GO synthesis through Hummers method. GO synthesized from this biochar was undistinguishable in structure and function from GO prepared from graphite as reported in all previous studies. The present investigation also investigated de-fluoridation of contaminated effluents by using biochar derived GO. The adsorption equilibrium data were satisfactorily fitted to the Langmuir adsorption model rather than Freundlich and Temkin isotherm model at different temperatures. The obtained experimental results were well fitted to pseudo–second order kinetic model. The nature of the adsorption mechanism was found to be endothermic and spontaneous in nature. Both response surface methodology and artificial neural network approach had been used to model the fluoride removal efficiency of GO. The optimization procedure showed good agreement between the predictive responses of the two models (RSM model and ANN model) with experimental results. As tea waste is cost-effective and environmentally safe, the synthesized GO from tea waste may be considered useful as an adsorbent for de-fluoridation of real time waste water as well.

Acknowledgment:

Authors would like to acknowledge the Department of Chemical Engineering, Jadavpur University, Kolkata, India and West Bengal Pollution Control Board, India for their support and service.

References:

Ahmad, M., Moon, D.H., Vithanage, M., et al., 2014. Production and use of biochar from buffalo-weed (Ambrosia trifida L.) for trichloroethylene removal from water. J. Chem. Technol. Biotechnol. 89, 150–157.

Alagumuthu, G., Rajan, M., 2010a. Equilibrium and kinetics of adsorption of fluoride onto zirconium impregnated cashew nut shell carbon. Chem. Eng. J. 158, 451–457.

Alagumuthu, G., Rajan, M., 2010b. Kinetic and equilibrium studies on fluoride removal by zirconium (IV): Impregnated groundnut shell carbon. Hem. Ind. 64, 295–304.

Alagumuthu, G., Veeraputhiran, V., Venkataraman, R., 2011. Fluoride sorption using Cynodon dactylon based activated carbon. Hem. Ind. 65, 23–35.

Asgari, G., Roshani, B., Ghanizadeh, G., 2012. The investigation of kinetic and isotherm of fluoride adsorption onto functionalize pumice stone. J. Hazard. Mater. 217–218.

Banerjee, P., Sau, S., Das, P., Mukhopadhayay, A., 2015. Optimization and modelling of synthetic azo dye wastewater treatment using Graphene oxide nanoplatelets: Characterization toxicity evaluation and optimization using Artificial Neural Network. Ecotoxicol. Environ. Saf. 119, 47–57.

Bhaumik, R., Mondal, N.K., Das, B., Roy, P., Pal, K.C., Das, C., Banerjee, A., Datta, J.K., 2012. Eggshell powder as an adsorbent for removal of fluoride from aqueous solution: Equilibrium, kinetic and thermodynamic studies. J. Chem 9, 1457–1480.

Botas, C., Álvarez, P., Blanco, C., Santamaria, R., Granda, M., Ares, P., Reinoso, F.R., Menéndez, R., 2012. The effect of the parent graphite on the structure of graphene oxide. Carbon 50, 275–282.

Chu, K.H., 2003. Prediction of two-metal biosorption equilibria using a neural network. European J. Mineral Proc. Environ. Prot. 3(1), 119-127.

Daifullah, A.A., Yakout, S.M., Elreefy, S.A., 2007. Adsorption of fluoride in aqueous solutions using KMnO4-modified activated carbon derived from steam pyrolysis of rice straw. J. Hazard. Mater.

147, 633–643.

Emmanuel, K.A., Ramaraju, K.A., Rambabu, G., Veerabhadra Rao, A., 2008. Removal of fluoride from drinking water with activated carbons prepared from HNO3 activation—A comparative study. Rasayan J. Chem. 1, 802–818.

Fan, X., Parker, D.J., Smith, M.D., 2003. Adsorption kinetics of fluoride on low cost materials. Water Res. 37, 4929–4937.

Garg, U.K., Kaur, M.P., Sud, D., Garg, V.K., 2009. Removal of hexavalent chromium from aqueous solution by adsorption on treated sugarcane bagasse using response surface methodological approach. Desalination, 249, 475–479.

Hamsaveni, D.R., Prapulla, S.G., Divakar, S., 2001. Response surface methodological approach for the synthesis of isobutyl butyrate. Proc. Biochem. 36, 1103–1109.

Hanumantharao, Y., Kishore, M., Ravindhranath, K., 2011. Preparation and development of adsorbent carbon from Acacia farnesiana for de-fluoridation. Int. J. Plant Anim. Environ. Sci. 1, 209–223.

Hernández-Montoya, V., Ramírez-Montoya, L.A., Bonilla-Petriciolet, A., Montes-Morán, M.A., 2012. Optimizing the removal of fluoride from water using new carbons obtained by modification of nut shell with a calcium solution from egg shell. Biochem. Eng. J. 62, 1–7.

Hu, B.B., Wang, K., Wu, L., Yu, S.H., Antonietti, M., Titirici, M.M., 2010. Engineering carbon materials from the hydrothermal carbonization process of biomass. Adv. Mater. 22, 813–828.

Hummers, W., Offeman, R, 1958. Preparation of Graphitic Oxide. J. Am. Chem. Soc. 80, 1339-1339.

Inagaki, M., Kim, Y.A., Endo, M., 2011. Graphene: preparation and structural perfection. J. Mater. Chem. 21, 3280–3294.

Jun, T.Y, Arumugam, S.D., Latif, N.H.A., Abdulla, A.M., Latif, P.A., 2010. Effect of activation temperature and heating duration on physical characteristics of activated carbon prepared from agriculture waste. Environ. Asia 3, 143-148.

Karthikeyan, G., Siva Ilango, S., 2007. Fluoride sorption using Morringa indica -based activated carbon. Iran. J. Enviton. Health Sci. Eng. 4, 21–28.

Kloss, S., Zehetner, F., Dellantonio, A., et al., 2012. Characterization of slow pyrolysis biochars: effects of feedstocks and pyrolysis temperature on biochar properties. J. Environ. Qual. 41, 990–1000.

Korbahti, B.K., Tanyolac, A., 2008. Electrochemical treatment of simulated textilewastewater with industrial components and Levafix Blue CA reactive dye: optimization through response surface methodology. J. Hazard. Mater. 151, 422–431.

Lee, S., Cho, S., Wong, M., 1998. Rainfall prediction using artificial neural networks. J. Geogr. Inform. Decis. Anal. 2 (2), 233–242.

Lehmann, J., Rillig, M.C., Thies, J., Masiello, C.A., Hockaday, W.C., Crowley, D., 2011. Biochar effects on soil biota-A review. Soil Biol. Biochem. 43, 1812–1836.

Li, Y., Zhang, P., Du, Q., Peng, X., Liu, T., Wang, Z., Xia, Y., Zhang, W., Wang, K., Zhu, H., et al., 2011. Adsorption of fluoride from aqueous solution by graphene. J. Colloid Interface Sci. 363, 348–354.

Lounici, H., Addour, L., Belhocine, D., Grib, H., Nicolas, S., Bariou, B., 1997. Study of a new technique for fluoride removal from water. Desalination 114, 241–251.

Ma, W., Ya, F.Q., Han, M., Wang, R.J., 2007. Characteristics of equilibrium, kinetics studies for adsorption of fluoride on magnetic-chitosan particle. J. Hazard. Mater. 143, 296–302.

Mohan, D., Rajput, S., Singh, V.K., et al., 2011. Modeling and evaluation of chromium remediation from water using low cost bio-char, a green adsorbent. J. Hazard. Mater. 188, 319–333.

Mohan, D., Sharma, R., Singh, V.K., et al., 2012. Fluoride removal from water using bio-char, a green waste, low-cost adsorbent: equilibrium uptake and sorption dynamics modeling. Ind. Eng. Chem. Res. 51, 900–914.

Roy, S., Das, P., 2016. Statistical optimization of defluoridation using novel activated carbon and cellulose from sugarcane bagasse: batch isotherm and kinetics study. J. Ind. Poll. Cont. 32(1), 368-380.

Roy, S., Das, P., 2016. Comparative analysis on treatment of fluoride containing solution using novel activated carbon prepared from lemon shell and wheat bran: Batch and column studies. Environ. Poll. Protec. 1, 40-53.

Sierra, U., Álvarez, P., Blanco, C., Granda, M., Santamaría, R., Menéndez, R., 2016. Cokes of different origin as precursors of graphene oxide. Fuel 166, 400–403.

Wu, Z., Ren, W., Gao, L., Liu, B., Jiang, C., Cheng, H., 2009. Synthesis of high-quality graphene with

a pre-determined number of layers. Carbon 47, 493–499.

Yetilmezsoy, K., Demirel, S., 2008. Artificial neural network (ANN) approach for modeling of Pb (II) adsorption from aqueous solution by Antep pistachio (Pistacia vera L.) shells. J. Hazar. Mater. 153(3), 1288-1300.

Yuan, J.H., Xu, R.K., Zhang, H., 2011. The forms of alkalis in the biochar produced from crop residues at different temperatures. Biores. Technol. 102, 3488–3497.